

## DESIGN AND EVALUATION OF NONLINEAR FOCUSED ULTRASONIC FIELD MAPPING AND MEASUREMENT SYSTEM

**Moad Essabbar<sup>1)</sup>, Gilles Despaux<sup>2)</sup>, Emmanuel Le Clézio<sup>2)</sup>**

1) *Euromed University of Fes, UEMF, Morocco*

(✉ [m.essabbar@insa.euromed.org](mailto:m.essabbar@insa.euromed.org) , )

2) *IES, University of Montpellier, CNRS, Montpellier, France*

### Abstract

Ultrasound plays a crucial role in various applications, including acoustic microscopy, medical imaging, therapy, and non-destructive testing. Despite its extensive use, experimental mapping of nonlinear focused ultrasonic fields is largely overlooked when compared to its linear counterparts or simulated nonlinear fields. The oversight arises from the inherent challenge of discerning electrical and acoustic nonlinearities. This research paper addresses this gap by proposing a 3D nonlinear ultrasonic field mapping system designed to provide precise measurements and imaging of both linear and purely acoustical nonlinear focused fields. The study involves initial simulations of linear and nonlinear ultrasonic fields emitted by a focused transducer in three dimensions. Subsequently, the proposed system is designed and experimentally validated through the acquisition of linear and nonlinear focused ultrasonic fields in two distinct fluids. The precision of the system is further demonstrated through the successful measurement of nonlinear parameters in the tested media, thereby contributing to the progression of nonlinear ultrasound field mapping and its applications.

Keywords: 3D field scan, nonlinear measurement, focused ultrasound, field mapping

### 1. Introduction

Ultrasonic measurement and characterization systems, such as scanning acoustic tanks and microscopes are based on the interaction of ultrahigh frequency sound waves with a material. Amplitudes, phases, and positions of reflected and/or transmitted ultrasonic waves are measured and computed, then used to construct images of the scanned zones [1, 2]. One of the strongest points of ultrasonic measurement systems is their ability to see through optically opaque surfaces, making it possible to get structural and properties information, not only from the surface but also of the internal structure of materials [3, 4].

Focused ultrasound measurement systems employ piezoelectric transducers that transform high-frequency electrical signals into acoustic waves that propagate at the same frequency. Advanced signal processing software and precision mechanisms are then used to scan the sample and

transform received ultrasonic data into high-precision pointwise characterization of the acoustic properties of the sample being scanned [5]. Ultrasonic measurements are generally done via the Reflection mode or Through-transmission mode. In the Reflection mode [6] (Fig. 2), a transducer emits a pulse, a burst or a continuous signal of ultrasonic waves, then the same transducer is used as a receiver to read the reflected waves. This technique is fairly often used due to its simple setup, requiring only one transducer. It also facilitates the inspection of materials because it only needs access to one side of the studied sample. The “Through-transmission” technique [7] (Fig. 1), however, uses two different ultrasonic transducers, one as an emitter and the other as a receiver. Homogeneous zones transmit ultrasound waves, while zones that present discontinuities prevent or weaken the propagation of sound waves, thus carrying additional information about the sample.

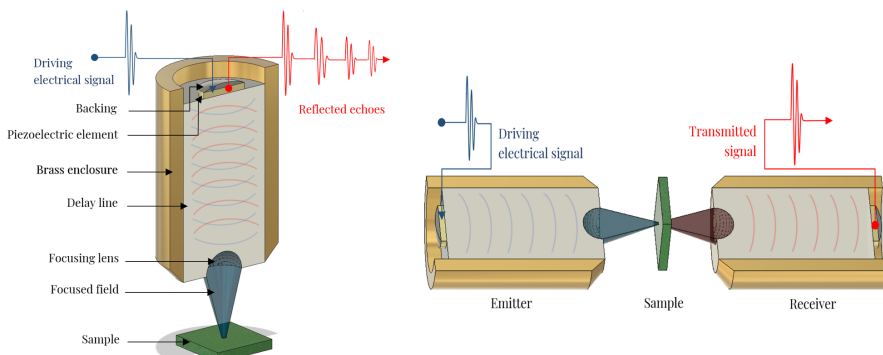


Fig. 1. Reflection (left) and Through-transmission (right) focused ultrasound measurement techniques.

In propagation media, the wavelength is defined as the ratio of the speed of sound in the media to the propagating wave frequency. This relation implies that the higher the frequency used, the shorter the wavelength in the media and therefore higher the resolution, by virtue of the Rayleigh criterion [8]. This is fundamental to nonlinear acoustic measurement since the generation of higher frequency harmonic fields created by nonlinear effects in media thus allows, if detected by a specifically designed reception system, an even better resolution to be achieved [9]. The nonlinear propagation of ultrasound offers a significant enhancement to the resolution of measurement and characterization systems. This phenomenon is particularly pronounced at high sound pressure levels, notably in focused ultrasound systems. In the context of this work, the nonlinear propagation of ultrasound is used to improve the resolution of the measurement system. The generation of higher frequency nonlinear fields in the medium allows for an even better resolution to be achieved, provided these harmonics can be detected by a specifically designed reception system. The nonlinear behaviour of the medium also provides additional information about the material properties, as different materials exhibit different degrees of nonlinearity. Therefore, by analysing the generated nonlinear fields, it is possible to gain additional information about the properties of the material, such as its nonlinearity parameter, which can be used for more accurate characterization of the material.

While extensive research has been conducted on linear focused waves [10], the experimental study of nonlinear focused waves remains an emerging field. Existing studies have primarily focused on simulations of nonlinear waves, with experimental mapping often focusing solely on axial intensity measurements [11]. Three-dimensional mapping of nonlinear focused fields provides a deeper understanding of nonlinear phenomena and leveraging advanced nonlinear ultrasound field focusing techniques.

## 2. Methods

### 2.1. Nonlinear propagation of ultrasonic waves

The linear theory of propagation of acoustic waves [12] considers the speed of sound waves in a medium to be constant. Accordingly, a mono-frequency acoustic wave does not deform during its propagation, although its amplitude may be reduced due to attenuation and diffraction. However, in nonlinear acoustics, the propagation speed of a wave changes depending on its particle speed and nonlinearity parameter B/A, which is used to describe the level of nonlinearity of materials. This parameter comes from the Taylor series expansion of variations of the pressure in a medium in terms of variation of density [13–15]. This nonlinearity phenomenon is described by Westervelt's equation [16] which accounts for nonlinearity up to the second order. Westervelt's equation (1) is as follows:

$$\left( \nabla^2 - \frac{1}{c_0^2} \frac{\partial^2}{\partial t^2} \right) p = -\frac{\delta}{c_0^4} \frac{\partial^3 p}{\partial t^3} - \frac{\beta}{\rho_0 c_0^4} \frac{\partial^2 p^2}{\partial t^2}, \quad (1)$$

where  $c_0$  is the sound velocity in the medium,  $p$  is the sound-wave pressure,  $\delta$  is the diffusivity parameter,  $\beta$  is the nonlinearity coefficient and  $\rho_0$  is the undisturbed mass density of the medium. On the left-hand side is a three-dimensional wave equation. The first term on the right-hand side represents diffusion and the second term represents nonlinearity. The particle velocity is represented by the ratio  $p \cdot (\rho_0 c_0)^{-1}$ . Cancelling the right-hand side terms will transform this equation into the classical three-dimensional linear wave equation.

In focused ultrasonic measurement systems, near the focus of the beam, the density variations produced by the wave may become significant enough to yield a faster propagation of the compressive part of the wave in comparison to the rarefactional one. As the ultrasound wave propagates, the nonlinearity will then distort the initially sinusoidal mono-frequency wave into a saw-tooth wave [17]. From the point of view of frequency spectrum, this transformation introduces harmonic frequencies [18] and constitutes the physical base of nonlinear ultrasound measurement and characterization.

### 2.2. Working principle of nonlinear focused ultrasound measurement

In linear ultrasonic characterization of materials [19], sound waves are transmitted and received at the same frequency; and due to the fact that resolution is frequency dependent, higher frequencies must be transmitted to achieve better resolution. This is not always possible due to attenuation, which also increases with frequency, making the wave unable to penetrate further through the sample [20]. An alternative method of improving the resolution is the usage of nonlinear properties of ultrasound propagation. Indeed, nonlinear sound propagation theory suggests that while propagating through a medium, mono-frequency waves are progressively distorted into a saw-tooth waveforms [21]. This transformation allows the generation of higher-frequency harmonic waves from a relatively low-frequency one, that, due to its low attenuation, can deeply propagate into the medium.

Experimentally, a mono-frequency wave is launched using a focused ultrasonic transducer. The choice of a focused transducer is determined by the small amplitude nature of nonlinearly generated harmonics. By using a focusing lens, it is possible to concentrate the ultrasonic waves in the focal zone to achieve a higher power than with a planar transducer. This allows the generation of more nonlinearity in the focal zone, creating higher-amplitude harmonics. At the reception, the signal is filtered, deleting the fundamental and keeping only the harmonic frequency that was generated during propagation. The information contained in the nonlinear field is collected to produce a nonlinear

measurement. One important challenge regarding this method is making sure that the transmitted signal is a pure mono-frequency wave, which is not simple because of all the nonlinearities that can be generated by the electronic components of the setup. Otherwise, the resulting measurement will merely be linear (not produced using the nonlinear fields generated in the medium).

### 3. Design and Simulation

While using the nonlinear ultrasound propagation model [22, 23], simulations of an XZ focused ultrasound field scan in water were implemented. In order to match the experimental specifications presented in the next section, a 3D concave source with dimensions matching those of the experimental transducers' lens (4.9 mm in radius and 5.58 mm in focal length) was created using the discrete model proposed by Martin [24]. For illustration, Fig. 2 presents a sampled down version of the focusing lens where independent voxels can be observed.

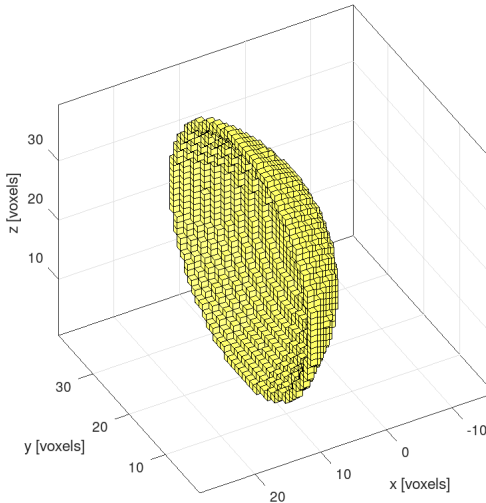


Fig. 2. Sampled down version of the 3D focusing lens.

The grid parameters were defined to get a maximum supported frequency of 28 MHz. The domain size was defined as a rectangular box with twice the lens's focal length for height and equal to the lens's diameter for the two remaining dimensions. Using these parameters, the simulation grid was composed of  $464 \times 411 \times 411$  grid points including a *perfectly matched layer* (PML). The calculations were performed using the nonlinear model of `kspaceFirstOrder3D` [25]. Despite being computationally demanding, the choice of a three-dimensional model makes it possible to better account for the focusing of the lens. The simulations were run on a server with sixteen-core Intel Xeon X5650 processors and 120 GB of memory available located at the Institute of Electronics and Systems – University of Montpellier.

The simulation outputs were recorded using a sensor mask that completely covered the XZ plane crossing the focal point to show the ultrasound field and match the experimental scan. Once the calculation in all grid points at all time steps is complete, each spatial point is analysed in the Fourier domain and the magnitudes of the present frequencies are extracted. Figure 3 represents zoomed views of the ultrasonic fields around the focal point at the fundamental frequency of 14 MHz and the harmonic frequency of 28 MHz, respectively. In agreement with the nonlinear

theory, the resulting field is found indeed to contain not only the fundamental frequency of 14 MHz but also a nonlinearly generated frequency of 28 MHz. At the fundamental frequency of 14 MHz, the ultrasonic field is generated linearly, and the size of the focal spot is relatively larger. This is a typical characteristic of linear ultrasonic fields, where energy is distributed over a broader area around the focal point. On the other hand, the harmonic frequency of 28 MHz represents the nonlinearly generated field. In this case, the focal spot is noticeably smaller. This is a key attribute of nonlinear ultrasonic fields, where energy is concentrated more tightly around the focal point due to the higher frequency. This concentration of energy results in a smaller focal spot, which can enhance the precision and resolution of the measurements.

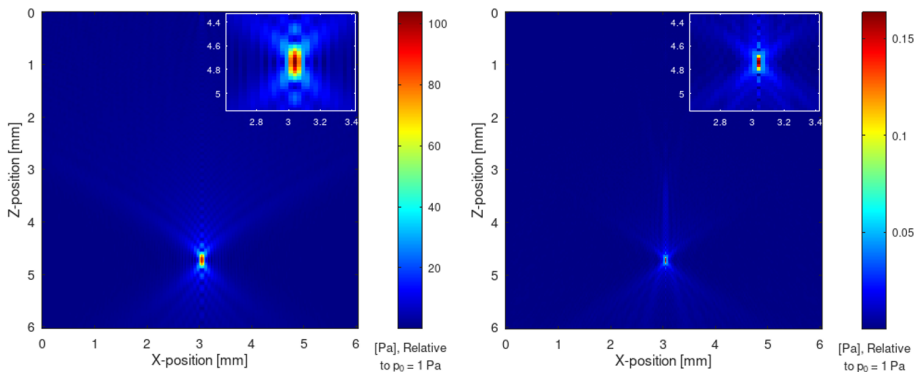


Fig. 3. 3D field simulation: zoomed view around the focal point at the fundamental frequency of 14 MHz (left) and at the harmonic frequency of 28 MHz (right).

#### 4. Experimental Setup

Nonlinear ultrasonic field mapping and measurement systems require very sensitive and vigorously tuned equipment compared to the classical linear counterpart. For nonlinear measurements, the transmitted power is higher, and the measured values are smaller in comparison with linear ones [26], thus further precision is required. An experimental bench was therefore set up to be used for detecting and mapping nonlinearly generated harmonic fields.

The experiments were performed in a  $38.5 \times 36 \times 33.3$  cm tank using a three-axis computer-controlled positioning system (Fig. 4) with an accuracy of 50 nm per axis. Three motorized axes were used to position a focused transducer that generates the ultrasonic waves.

The focused transducer (Fig. 5) uses a circular single-element lithium niobate as the piezoelectric crystal and a delay line made of silica, characterized by a sound velocity of 5830 m/s. The transducer has a frequency range centred around 14 MHz (Fig. 5), with a focusing lens of 5.59 mm in focal distance and 9.8 mm in diameter. The excitation signal, which is a continuous sine wave with an amplitude of up to 16 dBm, was programmed at a frequency of 14 MHz using an RF-Synthesizer. The transducer was designed and made at the Institute of Electronics and Systems of the University of Montpellier.

The transducer's bandwidth was chosen to be centred around the fundamental frequency of 14 MHz and insensible to the harmonic frequency of 28 MHz to ensure that the generated signals are purely nonlinear. For Scanning Acoustic Microscopy, this can be mitigated by using multi-element focused transducers in the reflection mode, with a spectral bandwidth divided for

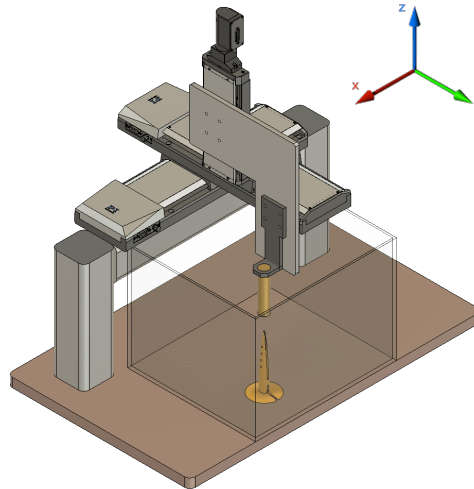


Fig. 4. 3D design of the experimental measurement setup.

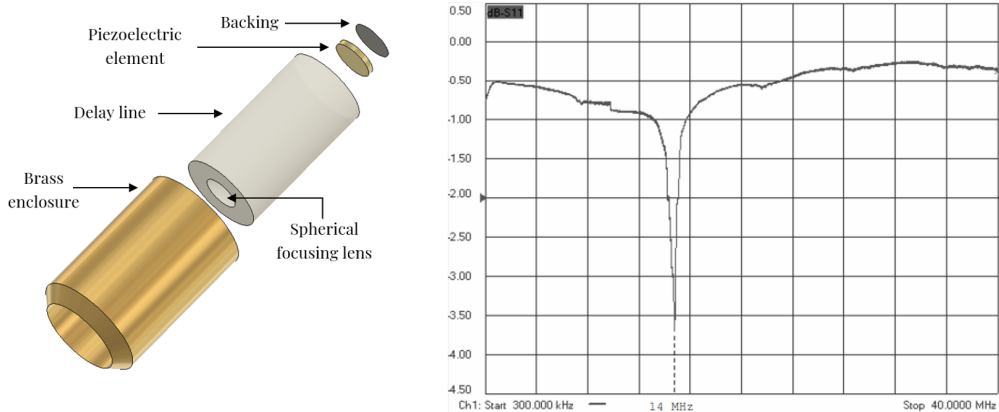


Fig. 5. Focused transducer design (left) and its Measured Reflection coefficient  $S11(\text{dB})$  (amplitude of the reflected wave to the incident wave) as a function of frequency (right).

transmission and for reception, or, in the transmission mode, by using multiple transducers with different non-overlapping bandwidths.

The receiver is a *polyvinylidene fluoride* (PVDF) needle hydrophone [27, 28] with an active element of 75  $\mu\text{m}$  diameter. Fig. 6 shows the end-of-cable,  $50 \Omega$  loaded sensitivity, along with its corresponding pre-amplifier. The data displayed in this figure was acquired by the National Physical Laboratory, London (NPL).

High-precision analogue tuneable bandpass filters were used with a cut-off frequency  $F_c$  of the 12–24 MHz range for the emitted signal at 14 MHz before driving the transmitter, and a filter with the 16–32 MHz  $F_c$  range for the received signal to extract the harmonic data from the hydrophone acquisition. Frequency domain signals at each spatial position were acquired using a spectrum analyser. Its high dynamic range and precise frequency measurement makes this device suitable as

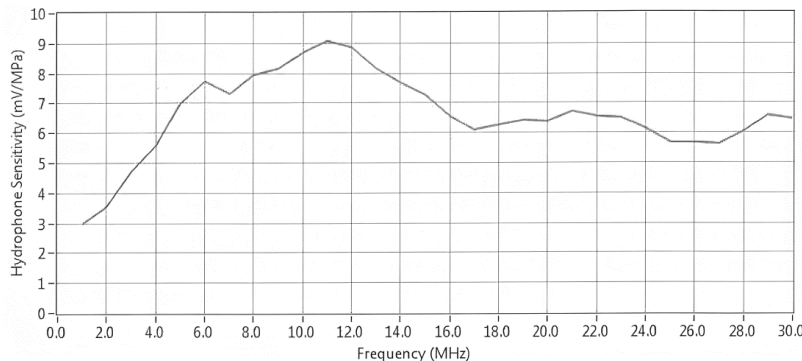


Fig. 6. Hydrophone sensitivity (mV/Pa) vs. frequency (MHz) for a system comprising a preamplifier, a DC Coupler and a 75  $\mu$ m needle hydrophone (data by Precision Acoustics ).

an acquisition system for mapping both linear and nonlinear fields. A LabVIEW program was finally developed to interface the hardware and perform the positioning, scanning, acquisition, and processing of the signals (Fig. 7).

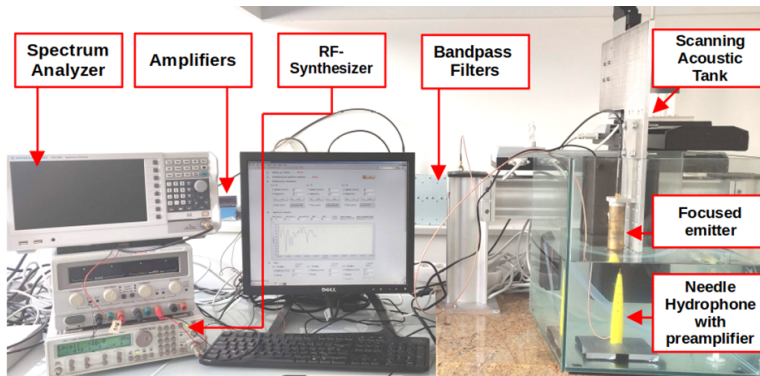


Fig. 7. Experimental measurement setup.

In addition to focusing, amplifying the transmitted source signal might be used to obtain higher-amplitude nonlinear harmonics. However, if not properly characterized, doing so would greatly compromise the reliability of the measurement system. Therefore, each electronic component was characterized in terms of input and output power at the fundamental and harmonic frequencies of 14 MHz and 28 MHz respectively. The system as a whole was found to be linear, not generating any detectable harmonic frequencies, for a source power up to 16 dBm, after which, the electronic components start to radiate harmonic frequencies that, unchecked, will merge with the nonlinearly generated acoustic harmonics and affect the accuracy of the measurement.

## 5. Results and Discussion

Using the aforementioned setup, nonlinear ultrasound propagation in two media, water and methanol, was investigated. The choice of these media is mainly due to the fact that, firstly, the values of their nonlinear parameters B/A are fairly different, allowing for a better evaluation of the

experimental setup and analysis of results. Secondly, these liquids are well documented in the literature, allowing comparison and validation of the methodology through the calculation of the parameter B/A. Scans of the focused acoustic fields were performed in the plane parallel to the beam axis (the XZ plane shown in Fig. 4) at the focal point.

### 5.1. Measured linear and nonlinear fields in water

Figure 8 presents the linear focused ultrasonic fields measured in water at the fundamental frequency of 14 MHz and at the harmonic frequency of 28 MHz, respectively. On the linear field scan, although the emitter is geometrically focused with a peak value of  $-24$  dBm at the focal point, the pressure level near the emitter's lens ( $z = 0$ ) is noticeable. This is due to the attenuation/distance relation. On the other hand, for the nonlinear field, no measurable pressure next to the lens is detected. This proves that the imaged nonlinear field is in fact not emitted by the transducer, but rather created due to nonlinear effects in the water. The nonlinearity begins to appear when the linear pressure is high enough during the propagation to generate strong harmonic waves in water, which starts at the near pre-focal region, thus creating a focused nonlinear pressure field that peaks at the focal point with a measured value of  $-118$  dBm.

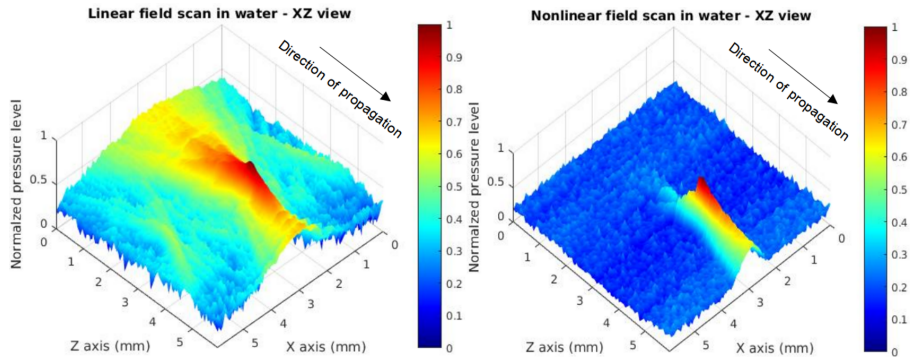


Fig. 8. Scanned focused ultrasonic fields in water: linear (14 MHz) field scan (left) and nonlinear (28 MHz) field scan (right).

This result holds significant importance as it validates the nonlinear nature of the observed pressure field. It also demonstrates the potential to produce harmonic frequencies in commonly utilized mediums like water, particularly at frequencies in the tens of MHz range, demonstrating the capability of the measurement system to accurately detect nonlinearly generated harmonics.

In the case of lateral distribution at the focal point (Fig. 7), the beam diameter of the nonlinear field is smaller than that of the linear one. The latter can be measured using the full width at half maximum of the field magnitude, where the field magnitude at the beam boundary is half of that at the focal point, yielding a beam diameter value of  $BD_F = 0.0823$  mm for the linear and  $BD_{2F} = 0.0376$  mm for the nonlinear field. These values can then be used to calculate the wavelength using (2) [29] where NA is the numerical aperture of the transducer:

$$\lambda \approx \frac{BD \times NA}{0.62}. \quad (2)$$

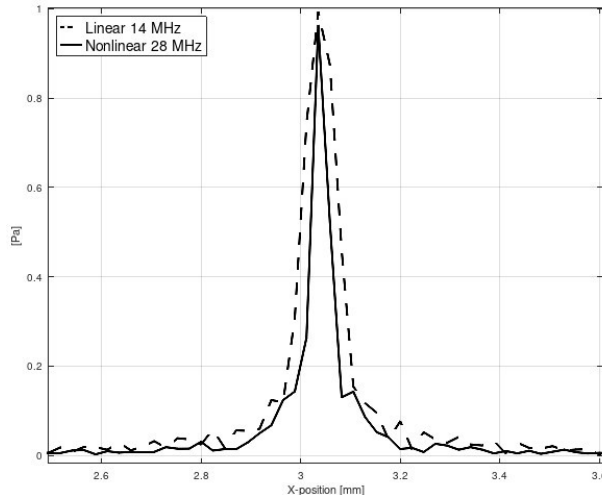


Fig. 9. Linear (14 MHz) and nonlinear (28 MHz) lateral pressure (normalized).

The resulting wavelength values are  $\lambda_F = 0.11$  mm and  $\lambda_{2F} = 0.05$  mm for the linear and the nonlinear fields, respectively. These values correspond to the theoretical values of wavelength for sound waves propagating in distilled water at the frequencies of 14 MHz and 28 MHz.

### 5.2. Measured linear and nonlinear fields in methanol

In the case of methanol, measurements of the pressure field were performed in the same experimental configuration as for water. Figure 8 shows the linear-focused ultrasonic field at the fundamental frequency of 14 MHz and the nonlinear-focused ultrasonic field at the harmonic frequency of 28 MHz, in pure methanol.

Comparing the two scanned fields, the nonlinear field is strictly generated in the media by the nonlinear propagation phenomenon as there is no measurable pressure near the lens and a maximal value of  $-122$  dBm at the focal point. It stands in contrast to the linear field where ultrasonic pressure is detected starting from the lens area and peaking in the focal zone with a measured value of  $-31.5$  dBm.

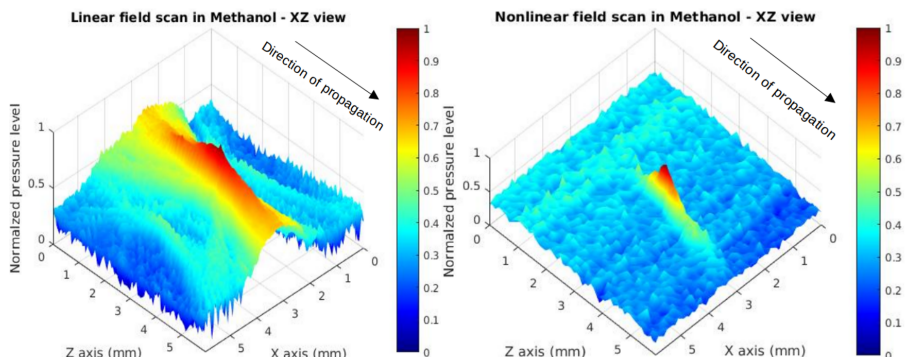


Fig. 10. Scanned ultrasonic focused fields in methanol: linear (14 MHz) field (left) and nonlinear (28 MHz) field (right)

These results enable a more precise characterization of a sample situated in the ultrasonic field's focal zone as well as extraction of the sample's nonlinear parameter. This is achieved by using a combination of the linear and nonlinear measurements as presented in the next section. Consequently, a higher measurement frequency (at least twice the original frequency) can be attained without the need for higher frequency transducers and suffering the attenuation counterpart, since, as demonstrated by prior scans, these nonlinear fields are entirely generated in the focal area.

### 5.3. Nonlinear parameter B/A

Since the previously described experimental setup is capable of measuring the pressure field within the focal zone, a finite amplitude model is suitable for estimating the nonlinearity coefficient B/A in this experimental configuration. The model proposed by Germain [30] predicts the harmonic power produced by the focused ultrasonic field as a function of the propagation medium parameters near the focal point using this equation:

$$\beta = \frac{P_2 \rho_0 c_0^5}{P_1^2 194\pi f_1^2 F^2 \exp\left(-7.1 \frac{c_0 F^2}{f_1} (2\alpha_1 + \alpha_2)\right)}, \quad (3)$$

where  $P_1$  is the power of the fundamental in the focal zone,  $P_2$  is the power of the harmonic in the focal zone,  $f$  is the frequency,  $F$  is the F-number of the lens, and  $\alpha_1$  and  $\alpha_2$  are the attenuation coefficients at the fundamental and harmonic frequencies, respectively. The nonlinear parameter B/A can then be found with the equation:

$$\beta = 1 + B/2A. \quad (4)$$

Using the pressure amplitudes of the previously measured linear and nonlinear fields in water and methanol, it is possible to calculate the nonlinearity coefficient using the (3) and (4) as well as the measured power of the fundamental and the harmonic waves in the focal zone.

Table 1 shows the final B/A coefficients obtained using the experimental setup measurements at 23°C. The values are successfully compared to the reference B/A parameters measured using different techniques, such as the frequency dependent finite-amplitude technique [31] and the thermodynamic technique [32]. These results, in addition to the previously imaged linear and nonlinear fields, further confirm that the measured nonlinear fields are completely generated due to the nonlinear acoustic propagation phenomenon in the medium, making this method suitable for both high resolution ultrasound field mapping and measurement systems as well as nonlinear characterization of fluid materials.

Table 1. Measured B/A in water and methanol.

Medium	Experimental B/A	Reference B/A
Water	$5.3 \pm 0.42$	$5.3^{[31]}$
Methanol	$10.2 \pm 0.82$	$9.6^{[32]}$

## 6. Conclusions

In order to accurately study focused nonlinear ultrasonic fields and increase acoustic characterization and measurement capabilities, an automated 3D nonlinear focused ultrasonic field mapping

and measurement system is designed and evaluated. The proposed scanning setup is capable of providing precise measurements and imaging of both linear and purely acoustical nonlinear focused fields. Furthermore, the system can be used to accurately measure the nonlinearity parameter B/A of different media, further confirming its measurement accuracy. The proposed system is evaluated by successfully comparing the measured nonlinearity parameter against different experimental methods as well as numerical simulations of the focused ultrasonic fields, accurately proving that the detected nonlinearities were solely those of the studied medium.

## 7. Future work

These results represent essential steps towards the development of a nonlinear/multi-frequency scanning acoustic measurement and material characterization setups, capable of inducing nonlinear generation in the sample placed in its focal zone and multi-spectral analysis of the received ultrasonic signals. Moreover, the nonlinear fields being fully generated in the focal area, this set-up allows local quantification of the nonlinear characteristics of the media.

As this work has focused on the study of the nonlinearity in homogeneous liquid samples, future works will then deal with its extension to the characterization of strongly nonlinear and heterogeneous media [33], placed in the ultrasonic field's focal zone. Heterogeneities exhibit higher degrees of nonlinearity, thus analysing the generated nonlinear fields would yield additional information about the material properties and structural details, making the system suitable for more accurate measurement and characterization, notably in the field of industrial *Non-Destructive Testing* (NDT) [34], where nonlinear acoustics can be key in overcoming important challenges in the field.

## References

- [1] Briggs, A., & Kolosov, O. (2009). *Acoustic Microscopy*. Oxford University Press.
- [2] Dwivedi, K., Trivedi, G., Khijwania, S., & Osuch, T. (2020). Design and numerical analysis of a highly sensitive ultrasonic acoustic sensor based on  $\pi$ -phase-shifted fiber Bragg grating and fiber Mach–Zehnder interferometer interrogation. *Metrology and Measurement Systems*, 27(2), 289–300. <https://doi.org/10.24425/mms.2020.132775>
- [3] Aghaei, A., Bochud, N., Rosi, G., Grossman, Q., Ruffoni, D., & Naili, S. (2022). Ultrasound characterization of bioinspired functionally graded soft-to-hard composites: Experiment and modeling. *The Journal of the Acoustical Society of America*, 151(3), 1490–1501. <https://doi.org/10.1121/10.0009630>
- [4] Lionetto, F. (2021). Ultrasound for Material Characterization and Processing. *Materials*, 14(14), 3891. <https://doi.org/10.3390/ma14143891>
- [5] Quate, C. F., Atalar, A., & Wickramasinghe, H. K. (1979). Acoustic microscopy with mechanical scanning – A review. *Proceedings of the IEEE*, 67(8), 1092–1114. <https://doi.org/10.1109/proc.1979.11406>
- [6] Wang, H., Yang, X., Liu, Y., Jiang, B., & Luo, Q. (2013). Reflection-mode optical-resolution photoacoustic microscopy based on a reflective objective. *Optics Express*, 21(20), 24210. <https://doi.org/10.1364/oe.21.024210>
- [7] Wearing, S. C., Kuhn, L., Pohl, T., Horstmann, T., & Brauner, T. (2020). Transmission-Mode Ultrasound for Monitoring the Instantaneous Elastic Modulus of the Achilles Tendon During Unilateral Submaximal Vertical Hopping. *Frontiers in Physiology*, 11. <https://doi.org/10.3389/fphys.2020.567641>

[8] Hingot, V., Chavignon, A., Heiles, B., & Couture, O. (2021). Measuring Image Resolution in Ultrasound Localization Microscopy. *IEEE Transactions on Medical Imaging*, 40(12), 3812–3819. <https://doi.org/10.1109/tmi.2021.3097150>

[9] Clair, B., Despaux, G., Chanson, B., & Thibaut, B. (2000). Utilisation de la microscopie acoustique pour l'étude des propriétés locales du bois: étude préliminaire de paramètres expérimentaux. *Annals of Forest Science*, 57(4), 335–343. <https://doi.org/10.1051/forest:2000124> (in French)

[10] Lean, H. Q., & Zhou, Y. (2019). Acoustic Field of Phased-Array Ultrasound Transducer with the Focus/Foci Shifting. *Journal of Medical and Biological Engineering*, 39(6), 919–931. <https://doi.org/10.1007/s40846-019-00464-z>

[11] Treeby, B. E., Wise, E. S., Kuklis, F., Jaros, J., & Cox, B. T. (2020). Nonlinear ultrasound simulation in an axisymmetric coordinate system using a  $k$ -space pseudospectral method. *The Journal of the Acoustical Society of America*, 148(4), 2288–2300. <https://doi.org/10.1121/10.0002177>

[12] Humphrey, V. F. (2007). Ultrasound and matter – Physical interactions. *Progress in Biophysics and Molecular Biology*, 93(1–3), 195–211. <https://doi.org/10.1016/j.pbiomolbio.2006.07.024>

[13] Hamilton, M. F., & Blackstock, D. T. (1998). *Nonlinear Acoustics* (1st ed.). Academic Press.

[14] Beyer, R. T. (1960). Parameter of Nonlinearity in Fluids. *The Journal of the Acoustical Society of America*, 32(6), 719–721. <https://doi.org/10.1121/1.1908195>

[15] Kielczyński, P., Szalewski, M., Balcerzak, A., Wieja, K., Rostocki, A. J., & Siegoczyński, R. M. (2013). Thermodynamic method for measuring the B/A nonlinear parameter under high pressure. *2013 IEEE International Ultrasonics Symposium (IUS)*, 1665–1667. <https://doi.org/10.1109/ultsym.2013.0424>

[16] Woodsum, H. C., & Westervelt, P. J. (1981). A general theory for the scattering of sound by sound. *Journal of Sound and Vibration*, 76(2), 179–186. [https://doi.org/10.1016/0022-460x\(81\)90350-3](https://doi.org/10.1016/0022-460x(81)90350-3)

[17] Blackstock, D. T. (1966). Connection between the Fay and Fubini Solutions for Plane Sound Waves of Finite Amplitude. *The Journal of the Acoustical Society of America*, 39(6), 1019–1026. <https://doi.org/10.1121/1.1909986>

[18] Shooter, J. A., Muir, T. G., & Blackstock, D. T. (1974). Acoustic saturation of spherical waves in water. *The Journal of the Acoustical Society of America*, 55(1), 54–62. <https://doi.org/10.1121/1.1919475>

[19] Anastasiadis, P., & Zinin, P. V. (2018). High-Frequency Time-Resolved Scanning Acoustic Microscopy for Biomedical Applications. *The Open Neuroimaging Journal*, 12(1), 69–85. <https://doi.org/10.2174/1874440001812010069>

[20] Waldner, C., & Hirn, U. (2020). Ultrasonic Liquid Penetration Measurement in Thin Sheets—Physical Mechanisms and Interpretation. *Materials*, 13(12), 2754. <https://doi.org/10.3390/ma13122754>

[21] Bjørnø, L. (2010). Introduction to nonlinear acoustics. *Physics Procedia*, 3(1), 5–16. <https://doi.org/10.1016/j.phpro.2010.01.003>

[22] Treeby, B. E., & Cox, B. T. (2010). k-Wave: MATLAB toolbox for the simulation and reconstruction of photoacoustic wave fields. *Journal of Biomedical Optics*, 15(2), 021314. <https://doi.org/10.1117/1.3360308>

[23] Treeby, B. E., Jaros, J., Rendell, A. P., & Cox, B. T. (2012). Modeling nonlinear ultrasound propagation in heterogeneous media with power law absorption using a  $k$ -space pseudospectral method. *The Journal of the Acoustical Society of America*, 131(6), 4324–4336. <https://doi.org/10.1121/1.4712021>

[24] Martin, E., Ling, Y. T., & Treeby, B. E. (2016). Simulating Focused Ultrasound Transducers Using Discrete Sources on Regular Cartesian Grids. *IEEE Transactions on Ultrasonics, Ferroelectrics, and Frequency Control*, 63(10), 1535–1542. <https://doi.org/10.1109/tuffc.2016.2600862>

[25] Treeby, B. E., & Cox, B. T. (2010). Modeling power law absorption and dispersion for acoustic propagation using the fractional Laplacian. *The Journal of the Acoustical Society of America*, 127(5), 2741–2748. <https://doi.org/10.1121/1.3377056>

[26] Rugar, D. (1984). Resolution beyond the diffraction limit in the acoustic microscope: A nonlinear effect. *Journal of Applied Physics*, 56(5), 1338–1346. <https://doi.org/10.1063/1.334124>

[27] Boechat, F. M. B., Rodrigues, E. P., de Oliveira, T. F., & Buiochi, F. (2018). Development of a PVDF needle-type hydrophone for measuring ultrasonic fields. *2018 13th IEEE International Conference on Industry Applications (INDUSCON)*, 1004–1007. <https://doi.org/10.1109/induscon.2018.8627232>

[28] Lin, Y., Shi, Y., Zhang, J., Wang, F., & Sun, H. (2020). Design and evaluation of a needle tip measurement system based on binocular vision. *Metrology and Measurement Systems*, 27(3), 495–512. <https://doi.org/10.24425/mms.2020.134593>

[29] Li, C., & Wang, L. V. (2008). High-numerical-aperture-based virtual point detectors for photoacoustic tomography. *Applied Physics Letters*, 93(3). <https://doi.org/10.1063/1.2963365>

[30] Germain, L., Jacques, R., & Cheeke, J. D. N. (1989). Acoustic microscopy applied to nonlinear characterization of biological media. *The Journal of the Acoustical Society of America*, 86(4), 1560–1565. <https://doi.org/10.1121/1.398716>

[31] Ehsan Jafarzadeh, Mohammad H. Amini, & Anthony N. Sinclair (2021). Determination of the Ultrasonic Non-linearity Parameter B/A versus Frequency for Water. *Ultrasound in Medicine & Biology*, 47(3), 809–819. <https://doi.org/10.1016/j.ultrasmedbio.2020.11.027>

[32] Garrett, S.L. (2020). Nonlinear Acoustics. In *Graduate Texts in Physics* (pp. 701–753). Springer International Publishing. [https://doi.org/10.1007/978-3-030-44787-8\\_15](https://doi.org/10.1007/978-3-030-44787-8_15)

[33] Xia, L. (2019). Analysis of acoustic nonlinearity parameter B/A in liquids containing ultrasound contrast agents. *The Journal of the Acoustical Society of America*, 146(2), 1394–1403. <https://doi.org/10.1121/1.5123486>

[34] Yadav, K., Yadav, S., & Dubey, P. K. (2022). Metrological investigation and calibration of reference standard block for ultrasonic non-destructive testing. *Metrology and Measurement Systems*, 29(3), 525–538. <https://doi.org/10.24425/mms.2022.142271>

**Moad Essabbar** received his M.Sc. degree in Embedded systems and Industrial IT from the National School of Applied Sciences in 2017. He received his Ph.D. degree in Electronics form the University of Montpellier in France in 2020 and is currently working as a Professor at Euromed University of Fes, Morocco. His research areas include embedded systems in biomedical applications, sensors and ultrasound microscopy.

**Emmanuel Le Clezio** graduated in Mathematics (1995) and Electronics (1997) from the University of Rennes 1, France, and earned a M.Sc. in Acoustics from the University of Le Mans in 1998. He completed his Ph.D. in Mechanics (Acoustics) at the University of Bordeaux 1 in 2001 and has been a Professor of Electronics at the University of Montpellier since 2011. Emmanuel le CLEZIO is a member of IEEE and the French Society of Acoustics. His research focuses on complex material characterization using ultrasonic methods.

**Gilles Despaux** graduated from the Engineering School in Robotics in 1990. He received his Ph. D. in Electrical Engineering in 1993 from the University of Montpellier 2. He is a member of the French Society of Acoustics, a member of IEEE, and has long been a member in scientific boards of numerous teaching and research national and international conferences. He is the author/co-author of more than 200 scientific publications and research reports. His research area includes material characterization and imaging by Acoustic Microscopy.